 CMC, vol.37, no.1, pp.59-75, 2013

Design of Aligned Carbon Nanotubes Structures Using Structural Mechanics Modeling Part 2: Aligned Carbon Nanotubes Structure Modeling

J. Joseph[1] **and Y. C. Lu**[1]

Abstract: The aligned carbon nanotube (A-CNT) structure is composed of arrays of individual CNTs grown vertically on a flat substrate. The overall structure and properties of an A-CNTs are highly dependent upon the designs of various architectures and geometric parameters. In Part 2, we have presented the detailed designs and modeling of various aligned carbon nanotube structures. It is found the A-CNT structures generally have much lower modulus than an individual CNT. The reason is due to the high porosity and low density of the A-CNT structures, since the interstitial space between nanotubes is mostly occupied by air. Increasing the nanotube array density is seen to have significantly improved the modulus of A-CNT structures. The mechanical property of the A-CNT structure can be affected by the individual nanotube atomic structure, but only at small wall thickness. As a material, the elastic modulus of the A-CNT is not affected by the size (height) of testing specimen.

Keywords: Aligned carbon nanotubes, Finite element method, Areal density, Mechanical properties.

1 Introduction

Practical applications often require that the carbon nanotube be produced in large scales and at oriented forms. These have resulted in an novel carbon nanotube material: the aligned carbon nanotube (A-CNTs) structures. The A-CNTs was first grown by Terrones et al. [Terrones et al. (1997)] through the method of laser ablation. In this experiment, a thin film of cobalt ($\sim$10–100 nm) was deposited on a silica plate. The coated plate was subsequently etched with a laser pulse to create linear tracks. Through the use of a patterned catalyst the aligned carbon nanotubes were formed. The aligned CNTs produced can have a length up to about 50 μm and a fairly uniform diameter of 30–50 nm. Since then, various techniques have been

[1] Department of Mechanical Engineering, University of Kentucky, Lexington, KY, U.S.A

used to synthesize this novel material. Li et al. (1999) have reported the growth of aligned carbon nanotubes by the pyrolysis of acetylene on an alumina template. In this method, the cobalt or nickel catalyst particles were pre-deposited at the bottom of the alumina membrane pores, followed by deposition of carbon nanotubes in the pores. The diameter, packing density, and length of carbon nanotube arrays could be tuned by altering the designs of the alumina templates. Recently, the chemical vapor deposition (CVD) method has been used to produce aligned CNTs. Dai and co-workers have prepared large-scale, aligned carbon nanotubes on the substrate surfaces by the pyrolysis of iron phthalocyanine (FePc) [Huang et al. (1999)]. Rao et al. (1998) and Wei et al. (2002) have synthesized well-aligned CNTs from ferrocene in xylene solution. Qu et al. have successfully produced aligned, single-walled carbon nanotube arrays by using the combined plasma-enhanced CVD and fast heating method [Qu et al. (2008)]. The single-walled A-CNTs are much lighter and more efficient than the multi-walled A-CNTs. A typical growth process for aligned carbon nanotube structures is shown in Fig.1.

As illustrated in Fig.1, an A-CNT structure is composed of arrays of individual CNTs grown vertically on a flat substrate. The overall structure of an A-CNTs highly depend upon the designs of various architectures and geometric parameters, including the tube height, tube diameter, tube array density, tube distribution pattern, inter-tube distance, tube-tube junction structure, and among many other factors. A small variation in each parameter would have great impact on the optimal performance of the A-CNT structure. Therefore, it is crucial to have a rational strategy to design and evaluate the architectures and geometric factors to help process the optimal nanotube materials. The traditional material development has relied on the experimental "trail-and-error" method, thus is a very slow and expensive process.The National Materials Advisory Board of the National Academy has recently recommended a brand new material development model to the entire material science community, i.e., the “Integrated Computational Materials Engineering (ICME)” [National Research Council (2008)]. The objective of the ICME approach is to integrate computational materials science tools into a holistic system that can accelerate materials development process. The most commonly used computational method for designing nanomaterials has been the atomistic approach, i.e., the classical molecular dynamics (MD), which has been very successful for modeling an individual nanotube. However, for an A-CNT structure that consists of millions or even billions of individual nanotubes, theatomistic approach is simply too computational expensive. The present papers present a frame work for designing and modeling the aligned carbon nanotubes structures by using thestructural mechanics approach, i.e., the finite element method. In Part 1, we have presented the fundamentals of the structural mechanics method and modeled the individual nanotube

- the fundamental building block of the aligned nanotube structures. In Part 2, we will present the detailed design and modeling of the aligned carbon nanotubes structures.

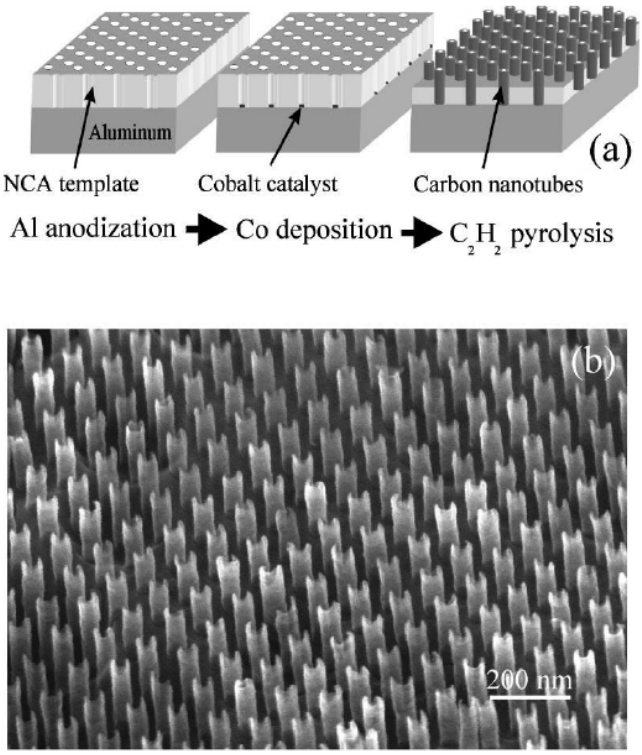

Figure 1: (a) Schematic showing the process of growing aligned carbon nanotubes structure. (b) SEM image of aligned carbon nanotubes structure. (Reprinted with permission from Appl. Phys. Lett. 75, 367 1999. Copyright 1999 American Institute of Physics.)

2 Modeling Procedures for Aligned Carbon Nanotubes Structures

The aligned carbon nanotubes structures are consisted of individual nanotubes that are packed vertically on flat substrates. The overall structures depend upon numerous geometric parameters, including tube array density, tube distribution pattern, inter-tube distance, tube-tube junction structure, among many others. To construct the A-CNT structures, the solid models forindividual carbon nanotubes in zigzag

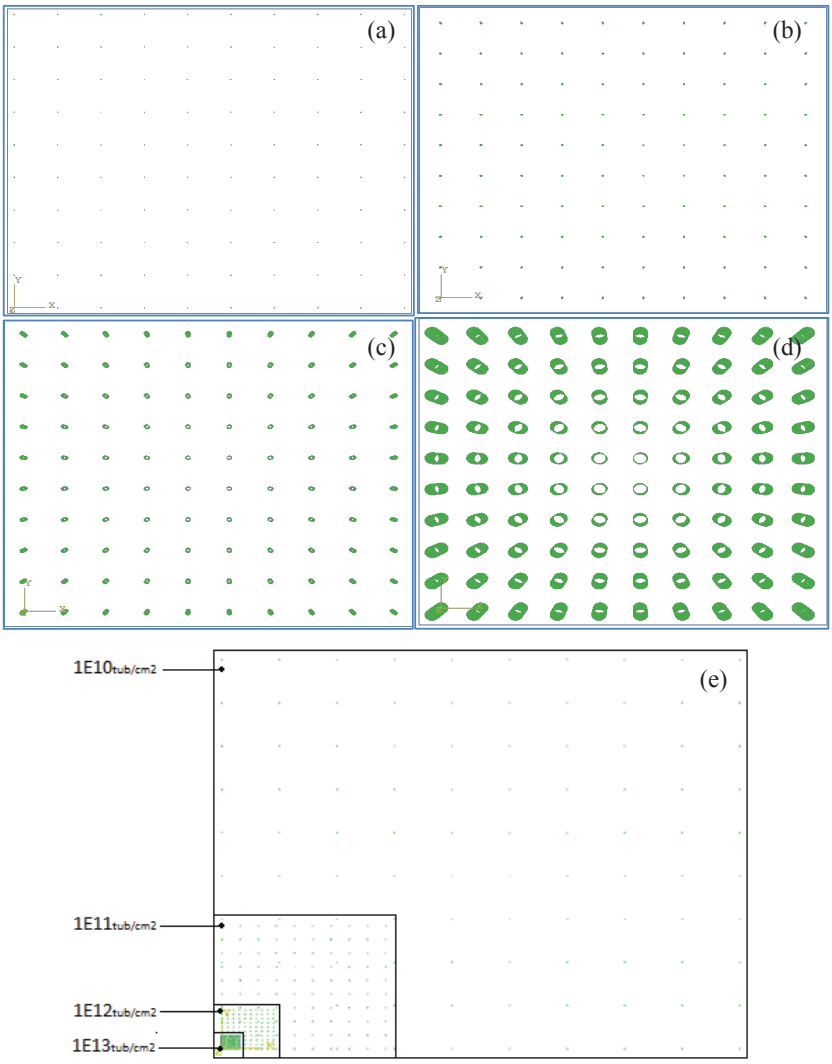

Figure 2: FE models of aligned carbon nanotubes structures at various tube densities: (a) $1x10^{10}$ tubes/cm^2, (b) $1x10^{11}$ tubes/cm^2, (c) $1x10^{12}$ tubes/cm^2, (d) $1x10^{13}$ tubes/cm^2, and (e) overview of A-CNT areal densities. The number of the tubes in the structure is 100 and height of the tube is 4.54 nm.

(a)

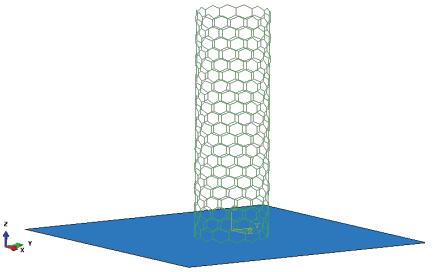

(b)

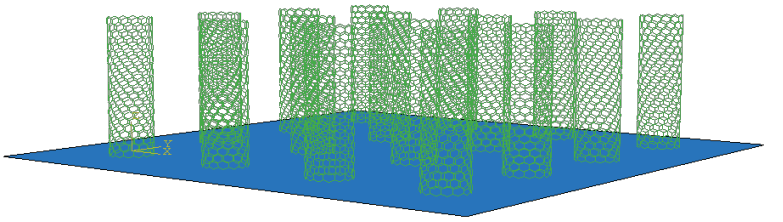

(c)

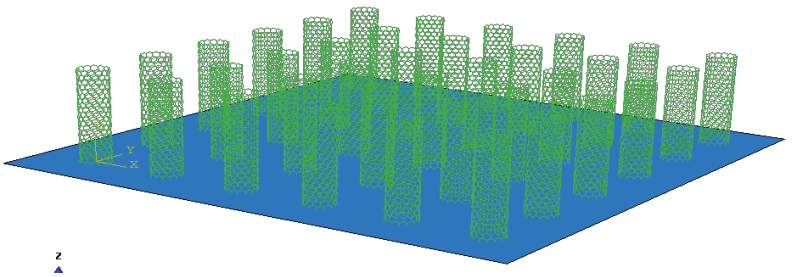

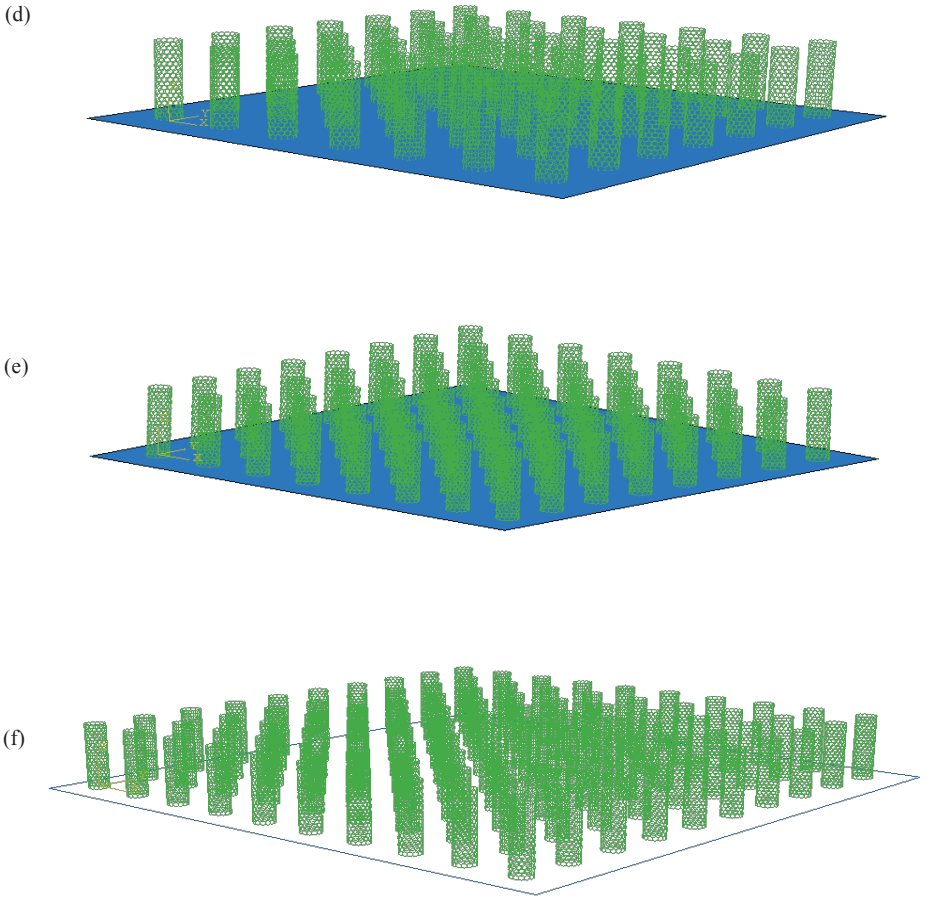

Figure 3: FE models of aligned carbon nanotubes structures containing different number of tubes: (a) 1 tube, (b) 16 tubes, (c) 36 tube, (d) 49 tubes, (e) 64 tubes, and (f)100 tubes. The height of the tube is 4.54 nm.

and arm chair configurations were geometrically modeled using the modeling capability of ANSYS software and then imported into ABAQUS CAE for FE modeling. The 3-node beam elements (B32) with a quadratic displacement function were used. Appropriate beam section orientation, geometric sectional properties, and material properties were assigned, following the procedures as described in Part 1. The A-CNT structures at various densities were constructed, ranging from $1x10^{10}$ tubes/cm^2 to $1x10^{13}$tubes/cm^2. FE models of various sizes, from 16-tube structure to 100-tube structure, were constructed. The heights of the A-CNT structures were varied, from 4.54 nm to 8.67 nm. To conduct compression experiments, the compression heads (as represented by analytical rigid surfaces) were subjected to various displacements in the downward direction. The bottom ends of the nanotubes were constrained in all directions to simulate the fixity of the nanotubes to the substrate material. Suitable contact interactions were defined between the nanotube top surfaces and the compression head surfaces with an assumed coefficient of friction of 0.1. Examples of the FE models for the vertically aligned carbon nanotubes structures are shown in Fig. 3 and Fig. 4.

3 Results and Discussion

3.1 Modulus of A-CNT Structures

An individeal carbon nanotube is believed to possess exceptionally high modulus and strength, with a Young's modulus as high as 1 TPa and a strength over 100 times of a steel [Krishnan et al. (1998); Wong et al. (1997); Lu (1997); Popov et al. (2000); Zhao and Shi (2011); Zeng (2011)]. However, the aligned nanotube array structures have been found to exhibit rather weak properties. The mechanical properties of the A-CNT structures have been experimentally investigated, mostly through the nanoindentation technique [Mesarovic et al. (2007); McCarter et al. (2006); Pathak et al. (2009); Patton et al. (2009); Zhang et al. (2010)]. The indenter used was either three-face pyramidal shape (Berkovich indenter), parabolic shape (spherical indenter), or flat shape (flat indenter). By driving the indenter into the specimen and then withdrawn from it, the indentation load-depth curves are obtained and then analyzed by following the standard Oliver-Pharr method [Oliver and Pharr (1992)]. The modulus of the A-CNT structures so determined have been found to vary greatly, ranging from several Megapascals to several hundred of Gigapascals (Tab. 1). The reason for the lower modulus is primarily due to the high porosity in the A-CNT structures, since the interstitial space between nanotubes is only occupied by air. In a typical A-CNT structure, the individual nanotubes are either completely separated from neighboring tubes or in weak contact with neighboring tubes through van der Waals attractions.

Table 1: Summary of Elastic Modulus of A-CNT Structures Determined through Various Nanoindentation Experiments.

Indenter Shapes Used in Indentation Experiments	**CNT Height**	**CNT Diameter**	**Elastic Modulus**	**References**
Flat Indenter	35-650 μm	10-20 nm	20-35 MPa	Maschmann et al. (2011); Lu et al. (2012)
Spherical Indenter	20μm, 500 μm	1-3 nm, 10 nm	18 GPa; 58 GPa	Misra et al. (2008); Zhang et al (2010)
3-Sided Pyramid Indenter	$\sim$ 600nm, 20μm	$\sim$ 50nm	0.9-1.2 TPa; 40-600 MPa; 0.1-0.8 GPa	Tong et al. (2008); Mesarovic et al. (2007)

In this study, the moduli of the A-CNT structures are evaluated through computational method. The construction and modeling of individual CNT have been discussed in detail in Part 1 of the paper. Assuming the same geometry and properties, those individual CNTs were arranged in various patterns and densities to construct the aligned carbon nanotube structures. Fig.4 shows the deformation of an A-CNT structure, in which the individual CNTs were arranged in an ordered square distribution in a small representative area (8.6E-4μm^2). The structure has an areal density of 10^{13} tubes/cm^2. Fig.5 shows the stress-strain response of this A-CNT structure. For comparison, the stress-strain response of a single CNT is also included. It is seen that the aligned CNT array has a noticeably lower stress-strain response, due to the open space between the tubes. The Young's modulus of the A-CNT structure is evaluated using Eq. 1. The resulting Young's modulus of the A-CNT array is approximately 0.103 TPa, which is about 12% of the modulus of a single CNT (0.79 TPa).

$$E = \frac{PL}{A\delta} \tag{1}$$

where

$P =$ Applied load

$\delta =$ Elongation of the nanotube

$L =$ Length of the nanotube

A = Cross sectional area of the nanotube

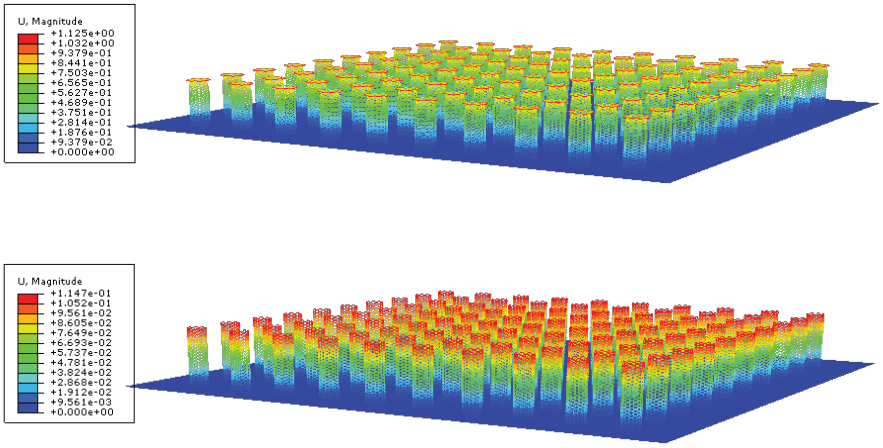

Figure 4: Deformation contours of aligned carbon nanotube structure under different compressions.

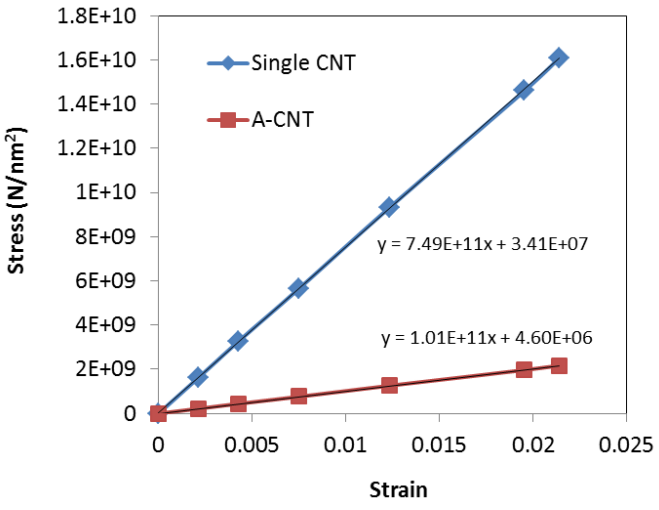

Figure 5: Stress-strain responses of individual CNT and A-CNT structure under compression.

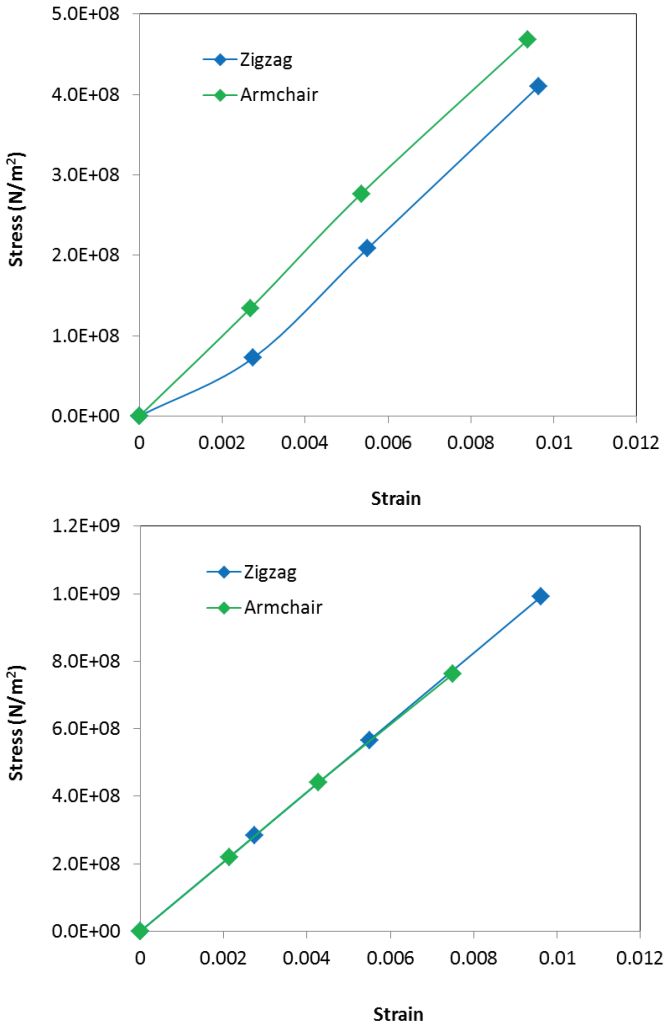

Figure 6: Comparison of stress-strain responses of two A-CNT structures with different atomic configurations. (a) The wall thickness of all individual tubes in the structure is 0.066 nm, and (b) The wall thickness of all individual tubes in the structure is 0.35 nm.

The effect of tube atomic structure on modulus of the A-CNT structures was further examined. Fig.6 shows the stress-strain responses of the A-CNT structures with zigzag and armchair configurations. It is observed that at thinner tube wall thickness (t=0.066 nm), there exists a noticeable difference in stress-strain curves between the two A-CNTs. The A-CNT in armchair configuration is much stiffer and has approximately 13% higher modulus than the A-CNT in zigzag configuration. When the tube wall thickness become larger (t=0.35 nm), the stress-strain curves of the two structures are almost indistinguishable and the Young's moduli of the two structures are essentially the same. The dependence of modulus on tube wall thickness is consistent with results observed earlier on single CNTs (Fig. 4 and Fig. 5 in Part 1).

3.2 Effect of FE Model Size

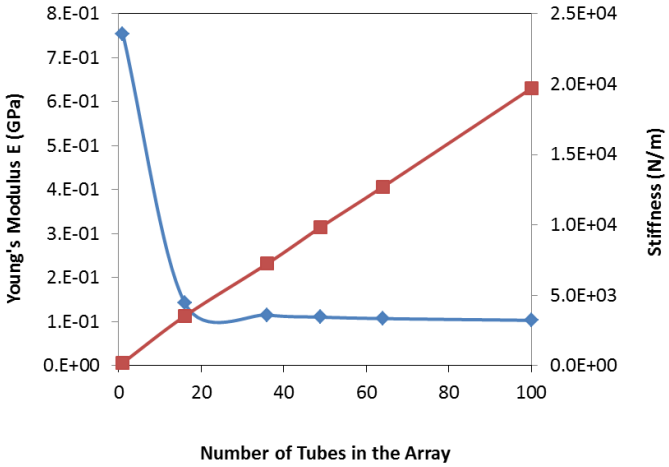

Figure 7: Effect of FE model size on properties of the A-CNT structure.

An aligned CNT structure contains millions of individual tubes per one square centimeters; therefore it is computationally impractical to consider all the tubes when design such structures. Here the A-CNT structures with various numbers of nanotubes (16-100) were constructed and then analyzed. Fig.7 shows the variations of stiffness and elastic modulus of the A-CNT structures as a function of the number of nanotubes. As expected, as the number of tubes in the structure increases, the stiffness increases. That is simply because there are more load-carrying members in the array. However, the modulus of the structures are seen to remain relatively constant as number of tubes increases. Thus, from design point of view, a modest

size FE model (>32 tubes) is sufficient for achieving accurate results while maintaining good computational efficiency.

3.3 *Effect of Tube Density*

The A-CNTs may be conceptually viewed as a complex structure consisted of nominally aligned tubes; between the tubes are unfilled open spaces that have no load-carrying capability. Therefore, the mechanical behaviors of the A-CNT structure are highly dependent upon the "density" of the nanotube arrays. A more densely packed nanotube array would have more load-carrying capability and fewer geometric freedoms for tube movements. Recent experimental study has shown that there exists a linear relationship between the elastic modulus of the A-CNT structure and its density. When the density of the A-CNT array is doubled, the modulus can be increased by 50% [Wardle et al. (2008)].

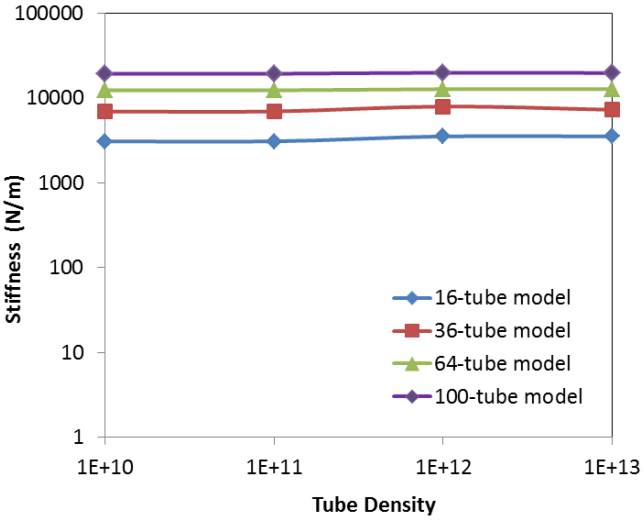

Figure 8: Effect of nanaotube areal density on stiffness of the A-CNT structures.

In present study, the A-CNT structures at various densities were constructed, ranging from $1x10^{10}$tubes/cm^2 to $1x10^{13}$tubes/cm^2. Fig. 8 and Fig. 9 show the results of these A-CNT arrays obtained with FE models containing 16 tubes to 100 tubes. In each model, it is seen that as the tube density increases, the stiffness remains relatively constant. This is because the overall number of the load-carrying structural members (tubes) remains the same in each array model (16 tubes, 32 tubes, 64 tubes or 100 tubes). However, the modulus is seen to increase linearly with the increase of the array density.

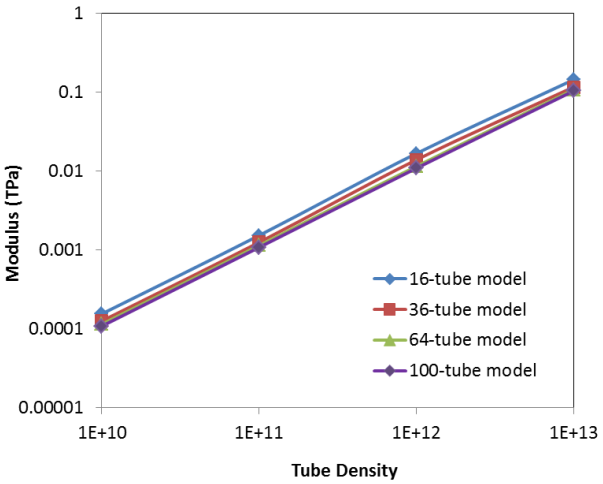

Figure 9: Effect of nanotube areal density on modulus of the A-CNT structures.

3.4 Effect of A-CNT Height

Although the aligned carbon nanotube arrays are initially grown on various substrates, they are able to retain their structural integrities after the removals of the substrates. Therefore, it has been widely accepted that an aligned carbon nanotubes is indeed a type of materials [Mesarovic et al. (2007); McCarter et al. (2006)]. As a material, the A-CNT will have its unique mechanical property (modulus), which should be independent upon the geometries of the testing specimens. Several researchers have examined the influence of nanotube length (height) on mechanical properties of the aligned carbon nanotube arrays, and have found that the elastic modulus remains relatively unchanged when the tube height varies [Tong et al. (2008); Maschmann et al. (2010)].

In this study, the A-CNTs with various lengths (heights) were modeled and the elastic modulus were evaluated. The nanotubes were all assumed in zigzag configuration with a fixed wall thickness of 0.34 nm. Fig.10 displays the resulted load-displacement curves of these A-CNT materials. As expected, the load-displacement responses clearly depend upon the specimen geometries. As the length of the A-CNT material is increased (from 4.54 nm to 8.67nm), the stiffness of the material has been reduced, from 3.5 N/mm to 7.1 N/mm.

The stress-strain curves of these A-CNT materials are shown in Fig.11. It is seen that the stress-strain responses of these materials are essentially indistinguishable. The modulus are computed, ranging from 110 GPa to 113 GPa, a merely 3% difference.

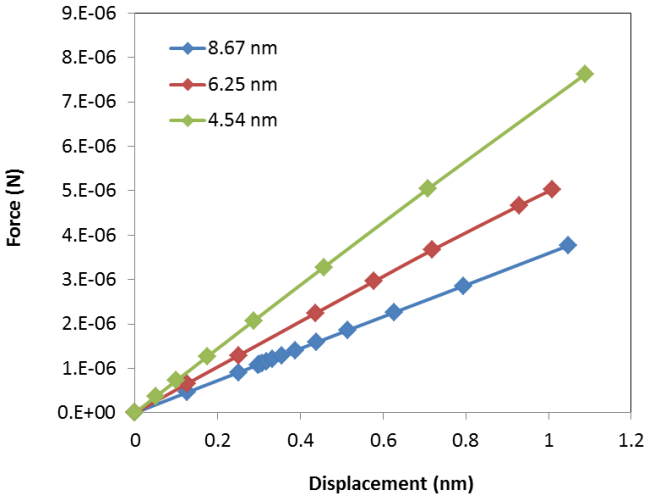

Figure 10: Load-displacement responses of the A-CNT structures at different heights. Results are obtained from the 36-tube A-CNT structure.

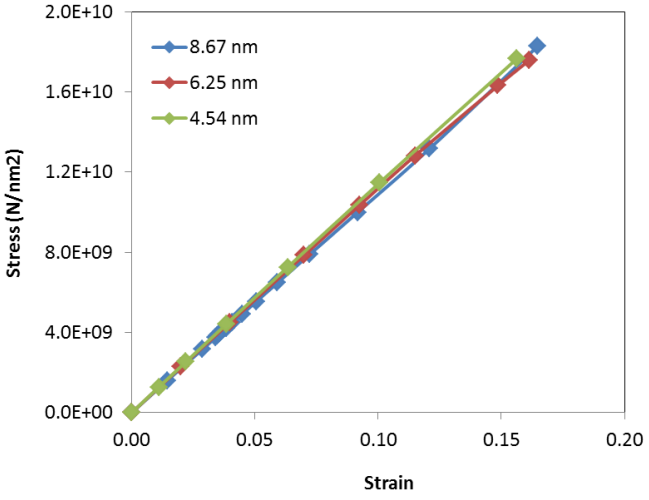

Figure 11: Stress-strain responses of the A-CNT structures at different heights. Results are obtained from the 36-tube A-CNT structure.

4 Summary

An attempt is made in this work to design and characterize the material properties of aligned carbon nanotube arrays by using structural-based finite element method. A-CNT structures with various densities and configurations have been constructed. Overall, the A-CNT structures exhibit much lower modulus than the individual CNT, due to their high porosities and low densities. By increasing the nanotube array density, the modulus of A-CNT structures are significantly improved. The individual nanotube atomic structure, i.e., zigzag versus armchair, can affect the mechanical property of the A-CNT structure, but only at small wall thickness. The elastic modulus of the A-CNT is not affected by the size (height) of testing specimen. The modeling approach serves as a computational tool to design and evaluate the architectures and geometric factors of the A-CNTs for further widespread applications in the automotive, aerospace, space and related industries and thus help process the optimal nanotube materials.

Acknowledgement

This work has been supported by the Kentucky NASA EPSCoR RIA program and the Kentucky Science and Engineering Foundation (KSEF) RDE program.

References

Huang, S.; Dai, L.; Mau, A. (1999) Patterned growth and contact transfer of well-aligned carbon nanotube films. *Journal of Physical Chemistry, B.*, vol. 103, pp. 4223-4227.

Li, J.; Papadopoulos, C.; Xu, J.; Moskovits, M. (1999) Highly-ordered carbon nanotube arrays for electronics applications. *Applied Physics Letters,* vol. 75, pp. 367-369.

Lu, J.P. (1997): Elastic properties of carbon nanotubes and nanoropes. *Physical Review Letters,* vol. 79, pp. 1297–1300.

Lu, Y.C.; Joseph, J.; Zhang, Q.; Dai, L.; Foster, D.C.; Baur., J. (2012): Large-displacement indentation of vertically aligned carbon nanotube arrays. *Experimental Mechanics,* vol. 52, no. 9, pp. 1551-1554.

Maschmann, M.R.; Zhang, Q.; Du, F.; Dai, L.; Baur, J. (2010): Length dependent foam-like response of axially indented vertically oriented carbon nanotube arrays. *Carbon,* vol. 49, pp. 386.

McCarter, C.M.; Richards, R.F.; Mesarovic, S. Dj.; Richards, C.D.; Bahr, D.F.; McClain, D.; Jiao, J. (2006): Mechanical compliance of photolithographically defined vertically aligned carbon nanotube turf. *Journal of Materials Science,*

vol. 41, pp. 7872–7878.

Mesarovic, S.D.; McCarter, C.M.; Bahr, D.F.; Radhakrishnan, H.; Richards, R.F.; Richards, C.D.; McClain, D.; Jiao, J. (2007): Mechanical behavior of a carbon nanotube turf. *Scripta Materialia,* vol. 56, pp. 157-160.

Misra, A.; Greer, J.R.; Daraio, C. (2008): Strain rate effects in the mechanical response of polymer-anchored carbon nanotube foams, *Advanced Materials*, vol. 20, pp. 1-5.

National Research Council (NRC). (2008): Integrated Computational Materials Engineering: A Transformational Discipline for Improved Competitiveness and National Security", Washington, D.C., The National Academies Press.

Pathak, S.; Cambaz, Z.G.; Kalidindi, S.R.; Swadener, J.G.; Gogotsi, Y. (2009): Viscoelasticity and high buckling stress of dense carbon nanotube brushes. *Carbon*, vol.47, no. 8, pp. 1969-1976.

Patton, S.T.; Zhang, Q.; Qu, L.; Dai. L.; Voevodin, A.A.; Baur, J. (2009): Electromechanical characterization of carbon nanotube grown on carbon fibers. *Journal of Applied Physics,* vol. 106, pp. 104313.

Oliver, W.C.; Pharr, G.M. (1992): An improved technique for determining hardness and elastic modulus using load and displacement sensing indentation experiments. *Journal of Materials Research*, vol. 7, pp. 1564.

Popov, V.N.; Van Doren, V.E.; Balkanski, M. (2000): Elastic properties of single-walled carbon nanotubes. *Physical Review B*, vol. 61, pp. 3078–3084.

Qu L.; Du F.; Dai L (2008): Preferential syntheses of semiconducting vertically aligned single-walled carbon nanotubes for direct use in FETs. *Nano Letters,* vol. 8, no. 9, pp. 2682-2687.

Rao C.; Sen R.; Satishkumar B.; Govindaraj A. (1998): Large aligned-nanotube bundles from ferrocene pyrolysis. *Chem. Commun*, pp. 1525-1526.

Tong, T.; Zhao, Y.; Delzeit, L.; Kashani, A.; Meyyappan, M.; Majumdar, A. (2008): Height independent compressive modulus of vertically aligned carbon nanotube arrays. *Nano Letters*, vol. 8, no. 2, pp. 511–5.

Treacy, M.M.J.; Ebbesen, T.W.; Gibson, J.M. (1996): Exceptionally high Young's modulus observed for individual carbon nanotubes. *Nature*, vol. 381, pp. 678–680.

Wardle, B.L.; Saito, D.S.; García, E.J.; Hart, A.J.; de Villoria, R.G.; Verploegen, E.A. (2008): Fabrication and Characterization of Ultrahigh-Volume- Fraction Aligned Carbon Nanotube–Polymer Composites. *Advanced Materials,* vol. 20, pp. 2707

Wei B.; Vajtai R.; Jung Y.; Ward J.; Zhang R.; Ramanath G.; Ajayan P (2002): Microfabrication technology: organized assembly of carbon nanotubes. *Nature*,

vol. 416, pp. 495-496.

Zhang, Q.; Lu, Y.C.; Du, F.; Dai, L.; Baur, J.; Foster, D.C. (2010): Viscoelastic creep of vertically aligned carbon nanotubes. *Journal of Physics, D: Applied Physics*, vol. 43, pp. 315401.

Zhao, P.: Shi, G. (2011): Study of Poisson Ratios of Single-Walled Carbon Nanotubes based on an Improved Molecular Structural Mechanics Model. *Computers Materials and Continua*, vol. 22, no. 2, pp. 147.

Zeng, X. (2011): Application of An Atomistic Field Theory to Nano/Micro Materials Modeling and Simulation. *Computer Modeling in Engineering and Sciences*, vol. 74, no. 3, pp. 183.